Available online at www.sciencedirect.com
SCIENCE DIRECT®
Surface Science 529 (2003) 223–230
SURFACE SCIENCE
www.elsevier.com/locate/susc

Formation of aluminum oxide thin films on FeAl(1 1 0) studied by STM

O. Kizilkaya [a], D.A. Hite [a,1], D.M. Zehner [b], P.T. Sprunger [a,*]

[a] *Department of Physics and Astronomy, Center for Advanced Microstructures and Devices, Louisiana State University, 6980 Jefferson Highway, Baton Rouge, LA 70803, USA*

[b] *Solid State Division, Oak Ridge National Laboratory, Oak Ridge, TN 37831, USA*

Received 14 November 2002; accepted for publication 6 February 2003

Abstract

The surface morphology and atomic structure of clean and oxidized FeAl(1 1 0) surfaces have been investigated with scanning tunneling microscopy (STM). An incommensurate reconstructed structure, having $FeAl_2$ stoichiometry confined to the outmost layer, is observed on the clean surface due to preferential Al segregation upon annealing to 1125 K. When the reconstructed clean surface is exposed to oxygen at elevated temperatures, an ordered ultra-thin aluminum oxide film is formed. Based on STM data, a structural model of the oxide film is proposed, which exhibits a quasi-hexagonal oxygen layer and accommodates an even mix of octahedral and tetrahedral occupancy of Al ions arranged in an alternating zigzag–stripe structure. STM imaging with tunnel voltages in the range of the bulk band gap implies that the thin film oxide electronic structure differs substantially from the bulk oxide, and indicates a local density of states around the oxide constituents within the bulk band gap.
© 2003 Elsevier Science B.V. All rights reserved.

Keywords: Aluminum; Iron; Metal–insulator interfaces; Scanning tunneling microscopy; Oxidation; Surface relaxation and reconstruction

1. Introduction

Due to their importance in a broad range of technological applications such as catalytic supports, microelectronics devices, and metal ceramic-based sensors, studies of oxide surfaces continue to draw considerable attention [1–3]. Among the oxides, alumina has been the focus of numerous studies due to its desirable physical and chemical properties. Bulk alumina gives rise to several phases, all of which are comprised of a close packed oxygen sublattice. The differences in occupancy of tetrahedral and/or octahedral coordination determine the crystal phase of alumina, and consequently, the overall properties. Despite years of investigation, developing a fundamental understanding of their complex surface/thin-film electronic and atomic properties has been hindered by the lack of high quality oxide surfaces that can be probed with standard surface/thin-film techniques.

* Corresponding author. Tel.: +1-225-5784621; fax: +1-225-5786954.
E-mail address: phils@lsu.edu (P.T. Sprunger).
[1] Present address: National Institute of Standards and Technology, Magnetic Technology Division, Boulder, CO 80305, USA.

0039-6028/03/$ - see front matter © 2003 Elsevier Science B.V. All rights reserved.
doi:10.1016/S0039-6028(03)00271-1

These experimental obstacles, including surface charging, can be minimized by the growth of ultra-thin oxide films on well-characterized metal substrates. Due to lattice mismatch effects, the production of alumina films from direct oxidation of aluminum results in morphologically rough surfaces and short-range crystallographic growth. However, previous studies have shown that ultra-thin alumina films, possessing long-range crystallographic structure have been successfully grown on other metal and alloy substrates.

Most notably, alumina growth on NiAl surfaces has been the subject of many studies, which have characterized the resulting dynamic, geometric and electronic structure of oxide surfaces, thin-films, and metal–oxide interfaces. Specifically, upon oxidation of clean alloy surfaces at elevated temperatures, different phases of well-ordered thin Al_2O_3 films have been identified on $Ni_3Al(1\,1\,1)$ [4,5], NiAl(1 1 1) [6,7] and NiAl(1 1 0) [8,9]. X-ray photoelectron spectroscopy (XPS), low energy electron diffraction (LEED) and scanning tunneling microscopy (STM) studies have demonstrated that a well-ordered 5 Å thick γ-Al_2O_3 film has been produced on NiAl(1 1 0) after dosing 1200 L of O_2 at elevated temperatures and annealing to 1150–1250 K for a short time. Two layers of oxygen and aluminum ions were proposed for these epitaxially grown oxides. High-resolution electron energy-loss spectroscopy experiments have confirmed that this oxide has γ-Al_2O_3 like, rather than α-Al_2O_3-like, structure, and is terminated with a hexagonal arrangement of oxygen ions [9]. Due to the symmetry of the substrate, two domains of oxide have been reported in accordance with STM images and LEED patterns [8,9].

Like NiAl, FeAl is also an ordered intermetallic alloy that crystallizes in the same CsCl-type crystal structure. In contrast to the well investigated oxidation behavior of NiAl(1 1 0), there are only preliminary Auger electron spectroscopy (AES), LEED and XPS studies of oxide films grown on FeAl(1 1 0) [10]. Graupner et al. reported that oxygen dosing at room temperature leads to the formation of amorphous Al_2O_3 with a thickness of ~5 Å. However, elevated temperature oxidation results in a well-ordered oxide film. LEED patterns for similarly oxidized NiAl(1 1 0) are also observed for FeAl(1 1 0), and XPS indicates that Al is the only cation in the oxide film, indicating formation of Al_2O_3, rather than any iron-oxide complex. Still, the detailed atomic and electronic structure of these oxide films has not been explored.

In the present paper, we report on an investigation of the nucleation, growth, and atomic structure of this ultra-thin oxide film grown on FeAl(1 1 0). In order to interpret the resulting oxide structure, STM results of the clean, high-temperature reconstructed phase of the FeAl(1 1 0) surface will also be presented. Because of strong similarities, the electronic and atomic structure of the resulting alumina film on FeAl(1 1 0) will be discussed in light of both experimental and theoretical results for aluminum oxide growth on NiAl(1 1 0) and other substrates.

2. Experimental details

The preliminary STM experiments were conducted at Oak Ridge National Laboratory using an Omicron® room temperature STM, followed by work completed at the Center for Advanced Microstructure and Devices at Louisiana State University, using a variable temperature STM, described in detail elsewhere [11]. Both STM measurements were performed in ultra-high vacuum chambers, equipped with LEED optics, cylindrical mirror analyzers for AES, as well as other surface cleaning/characterization instruments. The tunneling voltages refer to the bias on the sample with the tip at virtual ground. The lattice constant of the FeAl single crystal, grown at the Max Plank Institut fur Eisenforschung, was determined with X-ray diffraction to be 2.903 Å, corresponding to a constituency of $Fe_{0.53}Al_{0.47}$ [12]. This composition of the constituents prevents the phase transition, seen at 50–50% of the bulk alloy, between FeAl and $FeAl_2$ structures at low temperatures [13]. The (1 1 0) sample was aligned to $\pm 0.3°$ using Laue diffraction and mechanically polished [12]. The 5 mm diameter sample was mounted on a Ta sample platen with a K-type thermocouple attached to determine the sample temperature. The substrate was cleaned by repeated cycles of sputtering at

room temperature (Ne^+ ions, 1 keV, 20 μA), followed by e-beam annealing to 1125 K. The oxide thin film was prepared by dosing, at 1×10^{-6} Torr, the sample with oxygen, typically at 1125 K and consequently annealed for 5 min at this temperature.

3. Results and discussion

3.1. Atomic structure of the clean, reconstructed FeAl(1 1 0) surface

In stark contrast to NiAl surfaces, previous LEED and AES studies indicate that clean surfaces of low-index and vicinal surfaces of FeAl undergo surface reconstructions [14,15]. In the case of the (1 1 0) surface, it has been shown that preferential sputtering creates an attenuated Al concentration profile in the selvage region; however sequential annealing promotes aluminum segregation to the surface. Annealing to the temperature range of 1075–1175 K results in a surface reconstructed phase on the clean surface, which is the lowest energy configuration. Previous LEED studies by Graupner et al. [14] characterized the diffraction spots of the reconstructed surface as an incommensurate superstructure, which is commensurate in the $[1\,\bar{1}\,0]$ direction and incommensurate along the [0 0 1] direction of the FeAl (1 1 0) surface. In addition, their AES data indicate an enhanced concentration of aluminum at the surface, compared to the bulk composition. The surface concentration of Al was calculated to be 0.67 ± 0.06, corresponding to $FeAl_2$ surface stoichiometry assuming the segregated Al is confined to the topmost layer. They adopted a structural model of an ordered quasi-hexagonal overlayer which has a unit mesh containing two Al and one Fe atoms. This proposed surface structural model from LEED data has been corroborated by a more recent surface X-ray diffraction/reflectivity (XRD) study [16].

Correspondingly, the STM image, shown in Fig. 1a, reveals the atomic structure of this clean, incommensurate phase. STM images of the clean surface were acquired with tunneling currents between ±0.5 and ±5.5 nA, and bias voltages between ±30 mV and ±1 V. Variation of tunneling parameters (e.g. bias) did not appreciably change the observed structure. The STM results for this reconstructed FeAl(1 1 0) phase are consistent with the structural model determined from previous LEED and XRD studies [14,16], shown in Fig. 1b (for comparison, a bulk terminated surface ball

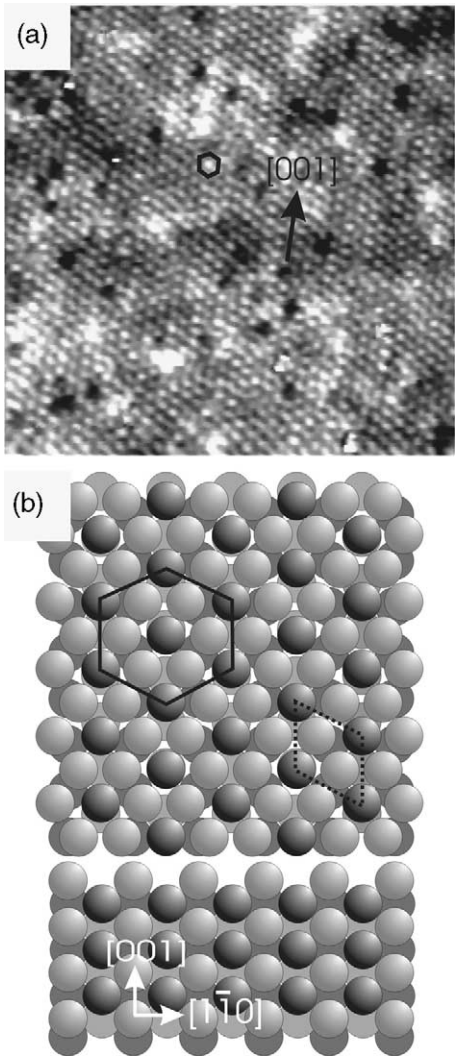

Fig. 1. (a) STM image (15×15 nm^2, $V_s = 30.2$ mV, $I_t = 5.4$ nA), acquired at room temperature, of clean FeAl(1 1 0) after annealing to 1125 K. The atomically resolved image shows Fe atoms surrounded by six Al atoms forming a $FeAl_2$ overlayer, as depicted in the hard ball model. (b) Dark balls represent Fe atoms with the unit cell indicated by a dashed line.

model is shown in the bottom of the model). As seen in the model, a quasi-hexagonal arrangement of atoms is atomically resolved in the STM image. The hexagon mesh drawn with a solid line in the ball model implies that the imaged atoms are Fe, surrounded by six Al atoms. The unit mesh, shown with a dashed line adopting the 1:2 ratio of Fe:Al, confirms the $FeAl_2$ stoichiometry. The measured distance of 8.22 Å between two successive Fe atoms in the [1 $\bar{1}$ 0] direction of substrate confirms the commensurability; however, the periodicity along the [0 0 1] direction (4.2 ± 0.05 Å) lacks commensurability with the underlying substrate (2.9 Å). Upon oxygen exposure at high temperatures, this reconstructed surface becomes the template for nucleation and growth of well-ordered ultra-thin alumina films.

3.2. Atomic and electronic properties of alumina thin films on FeAl(1 1 0)

Ultimately, the composition and structure of the oxide that forms on FeAl is dictated by the overall energetics. Since the enthalpy of formation of Al_2O_3 ($\Delta H_f = -1676$ kJ/mol) is lower than that for Fe based oxides ($Fe_2O_3 = -826$ kJ/mol, $FeO = -278$ kJ/mol, $Fe_3O_4 = -1118.4$ kJ/mol) [17], it is thermodynamically more favorable that aluminum be preferentially oxidized on the FeAl-(1 1 0) surface forming an ultra-thin Al_2O_3 film. From previous experimental studies [10], it is known that the oxidation of FeAl(1 1 0) can result in three different structural phases, as determined by LEED, of alumina films on the surface, depending on the substrate temperature during oxygen exposure. Although an amorphous Al_2O_3 structure is formed at temperatures up to 775 K primarily due to kinetic limitations, a "streaked oxide" phase with short-range order is observed with a saturation exposure of oxygen within the 775–975 K temperature range. Tentatively, the structure of this latter oxide phase is related to the missing-row reconstructed FeAl(1 1 0) surface that occurs within this temperature range.

As opposed to these lower temperature phases, a well-ordered aluminum oxide phase can be produced at or above 1125 K and is the primary focus of this STM study. Fig. 2a shows a large-scale STM image that reveals the overall structure and morphology of this high-temperature phase of ultra-thin alumina formed on reconstructed FeAl-(1 1 0), upon exposure of 1000 L of O_2 (i.e. saturation coverage) at 1125 K. The large-area STM image, acquired after the exposed sample was recooled to room temperature, shows a periodic and nearly hexagonal superstructure on the ordered oxide. The spot-to-spot distance of the superstructure is approximately 19 Å. STM images reveal that with saturation coverages (as in Fig. 2a), the thin-film alumina grows homogeneously across the surface in a relatively flat morphology with a lateral disorder primarily perpendicular to the [0 0 1] direction. LEED confirms this disorder, with streaking along the [1 $\bar{1}$ 0] direction. The unit cell of the oxide film (18.6 × 19.4 $Å^2$), shown by a solid line, is much larger than that of the substrate (2.9 × 4.1 $Å^2$), and is rotated by 30° with respect to the [1 $\bar{1}$ 0] direction of substrate. Due to the two-fold symmetry of the substrate, two rotational domains are expected and are indeed observed for the aluminum oxide on NiAl(1 1 0) [9,18]. However, as in the case of STM studies of Al_2O_3/Ni_3Al(1 1 1) [5], our STM data reveals only one domain in the present case. The measured corrugation height is 0.55 ± 0.05 Å; this large value is not solely due to variations in the structural morphology, but also includes strong lateral variations in the local electronic structure.

The STM image in Fig. 2b reveals large homogeneous films separated by a step edge. In the present case, the measured step height is ~8 Å (see linescan at the bottom of figure). It is believed that this height corresponds to a large step in the underlying metal substrate; STM images of the clean FeAl(1 1 0) surface reveals step heights of 2–8 Å. Only a few defects in the oxide film are observed. Typically they are imaged as "holes" as identified by the arrow in Fig. 2b. If it is assumed that this hole indicates a lack of oxide growth, then the measured depth should be indicative of the thin-film oxide thickness. As seen in the linescan, the depth of the hole, employing the given tunneling parameters, is ~4 Å; previous LEED studies of this system determine the thickness to be ~6 Å [10]. Although quite similar, it is acknowledged that the measured depth of the hole with STM

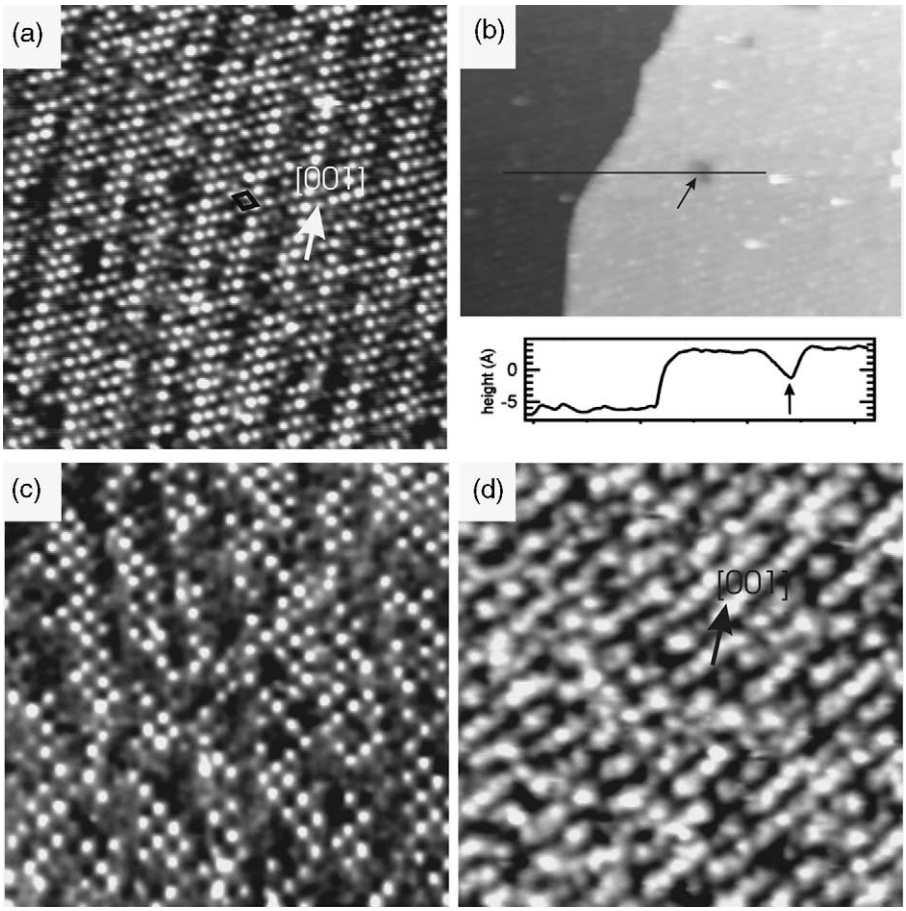

Fig. 2. (a) STM image (70×70 nm^2, $V_s = -1.25$ V, $I_t = -0.7$ nA) of oxidized FeAl(1 1 0) after exposure of 1000 L of O_2 (saturation). A unit mesh (18.6×19.6 Å^2) is displayed with a solid line. Propensity of ordering along the close packed direction of the substrate is observed. (b) STM image (69×100 nm^2, $V_s = 1.25$ V, $I_t = 0.17$ nA) shows a step edge and void hole formation, marked by an arrow. Line scan, below the image, indicates a step height (~8 Å) and nanoscale hole formation (4 Å depth width and 80 Å across). (c) Low coverage of O_2 exposure (125 L) reveals local order with a larger unit cell than the saturated surface (72×72 nm^2, $V_s = -0.4$ V, $I_t = -3.69$ nA). (d) STM image (50×50 nm^2, $V_s = 3.02$ V, $I_t = 1.04$ nA), total exposure of 1000 L, reveals an electronic structure effect, showing a line pattern with positive bias voltage.

may not accurately represent the true oxide thickness due to electronic effects. For example, from previous studies on the NiAl(1 1 0) substrate, it is known that apparent height of oxide step edges and hole defects depends critically on tunneling parameters [18,19]. However, in these studies the apparent height attenuated when tunneling bias values within the "gap" were employed. In contrast, we do not observe this effect.

Subsaturation coverages of oxygen at 1125 K results in an oxide superstructure that lacks long-range order. Fig. 2c shows an image of the surface produced with an exposure of only 125 L. The spot-to-spot distance is, on average, larger than on the saturated surface. Because of the somewhat disordered surface, STM does not yield direct information about the oxide structure of the subsaturated alumina film. However, LEED reveals that, in addition to the oxide superstructure, incommensurate diffraction spots corresponding to the clean reconstructed FeAl(1 1 0) surface are concurrently observed. This implies that while

short-range order of the oxide film is maintained, either patches of clean FeAl(1 1 0) or a non-equilibrium structure of oxide exists. Higher exposure of oxygen (corresponding to Fig. 2a) results in the disappearance of the incommensurate hexagonal diffraction spots, indicating the interfacial layer between the oxide thin film and substrate does not maintain its reconstructed structure. XPS data [10] imply that the presence of a smaller Al 2p peak, in addition to the major one, is indicative of Al atoms between the oxide and the substrate. As corroborated by STM data, the disappearance of intense superstructure diffraction spots in the LEED pattern demonstrates that the ultra-thin film of aluminum oxide extends homogeneously across the surface at saturation coverage.

In order to investigate the influence of the oxide electronic structure on STM images, data were acquired under reverse bias conditions. Fig. 2d shows an image of the saturated oxide film acquired with +3 V bias voltage (opposite tunneling polarity compared to the one used in Fig. 2a and c). As seen, tunneling with positive sample bias voltage reveals a different electronic configuration showing a line pattern structure of the oxide. The lines, with a periodicity of nearly 30 Å, are rotated approximately 40° with respect to the [0 0 1] direction. The apparent structural changes seen with opposite tunneling polarity are produced by electronic band structure effects of the oxide film. Since the unoccupied bands may have a different density of states and symmetry, changing the bias voltage may result in tunneling into different states, whose symmetries differ from those of the occupied bands. We assert that the difference in the local electronic structure, i.e. density of states and symmetry of the un/occupied bands, results in a substantial difference in the apparent morphology with different polarity. The structure of the oxide, shown in Fig. 2d with positive polarity, is very similar to the STM/AFM results of NiAl(1 1 0) [20].

In earlier studies on Al_2O_3/NiAl(1 1 0) [9,19], it was argued that due to the wide band gap of the bulk oxide (8 eV), STM images obtained by tunneling in this gap correspond to the contributions from both the oxide and, more importantly, from the interfacial electronic structure. That is, the atomic structure of the oxide surface is only revealed upon tunneling into (out of) conductance (valence) states. However, this assumes that the electronic properties of the thin film have direct analogs to the bulk oxide. A recent theoretical study by Jennison et al. [21] of supported alumina thin films determined a non-zero local density of states (LDOS) of aluminum and oxygen within the expected bulk band gap. This result is a consequence of the film thickness and the expected quantum mechanical mixing of the non-bulk-like chemical environment within the oxide layers. Similarly, it is believed that due to the unique atomic and chemical structure of ultra-thin Al_2O_3 films grown on FeAl(1 1 0), STM can indeed be used to elucidate the surface atomic structure of the Al–O thin film. However, the results are best interpreted with information about the bulk structure and theoretical predictions focused on the ultra-thin films.

The structure of bulk γ-Al_2O_3 has been a matter of discussion for nearly 40 years. The debate mainly stems from questions regarding the position of vacancies required for charge balance in the defect structure. Most experimental studies [22,23] suggest that a small number of cations occupy tetrahedral sites, whereas the normal preference for Al ions is considered to be in octahedral sites. However, a recent transmission electron diffraction study [24] has revealed a reverse assessment, indicating all tetrahedral sites are occupied by cations and vacancies are found at the octahedral sites. Again, these controversial findings correspond to the *bulk* structure.

Regarding the ultra-thin alumina films, although experimental studies have not adequately addressed the question of the coordination of Al ions, ab initio calculations have revealed much as to the atomic structure of the thin film Al_2O_3 and corresponding electronic structure [21]. Specifically, calculations performed on simulated 5 Å Al_2O_3 films, supported on Al(1 1 1), Mo(1 1 0) and Ru(0 0 0 1) substrates, have demonstrated that the tetrahedrally coordinated Al^{3+} ions are located nearly in the same plane as the oxygen ions for electroneutrality. These calculations concluded that an overall structure composed of two oxide layers, wherein the Al ions are tetrahedrally co-

ordinated to O ions, describe the lowest energy configuration. Even though the occupied density of states of the bulk oxide begins at about 4 eV below the Fermi energy, they calculated that a non-zero LDOS from aluminum and oxygen for the two oxide layers lie within the bulk band gap of the oxide. Due to this finite LDOS near E_F, at small tunnel voltages, we tentatively propose that STM directly reveals the atomic structure of the thin film.

Considering a larger unit cell [25], Jennison et al. recently showed a propensity of an even mix of tetrahedral and octahedral site Al cations, constituting the lowest energy stable film. The resulting structure is composed of an alternating zigzag structure of equal number of tetrahedral and octahedral Al ions with an increase in the interlayer Al–Al spacing. They also described a structure consisting of an alternating stripe and zigzag structure, but due to a decrease in the Al–Al separation resulting in higher energy, this structure is not favored. In Fig. 3a, a well-ordered structure consisting of a composite zigzag and stripe structure, alternating every two atoms along the [0 0 1] direction of the substrate, is clearly seen. Based on the similarities with the theoretical model [25], we propose that the atomic topography observed here with STM is due to Al ions that are assumed to be coplanar with oxygen atoms. The ball model at the top of Fig. 3b depicts this proposed structure. For comparison, the bottom part of Fig. 3b shows the pure octahedral arrangement of Al ions, consistent with a bulk Al_2O_3 arrangement (see unit cell at bottom). Relative to the unit cell of bulk Al_2O_3, the resulting surface structure adopted from these STM measurements is consistent with a larger unit cell. Although not definitive, the unit cell shown at the top of Fig. 3b reveals a (4×2) structure with respect to the bulk-oxide unit cell and is consistent, both rotationally and spatially, with the quasi-hexagonal superstructure observed in the STM image of Fig. 2a. Assuming this model is valid, the occupancy of cations in tetrahedral sites is equal to that of octahedral sites, and questions the assumption of a surface Al_2O_3 stoichiometry. However, some questions still remain concerning this proposed structure. For example, atomically resolved STM images of the superstructure are needed to confirm the model. Indeed, assuming an attenuated Al occupancy in the surface layer, in order to maintain proper stoichiometry, periodic oxygen vacancies may be present, perhaps oriented along the [0 0 1] direction of substrate. Because we were unable to obtain atomically resolved images to determine quantitative vacancy ratios of the outmost layer, this model is only tentative and calls upon additional theoretical input.

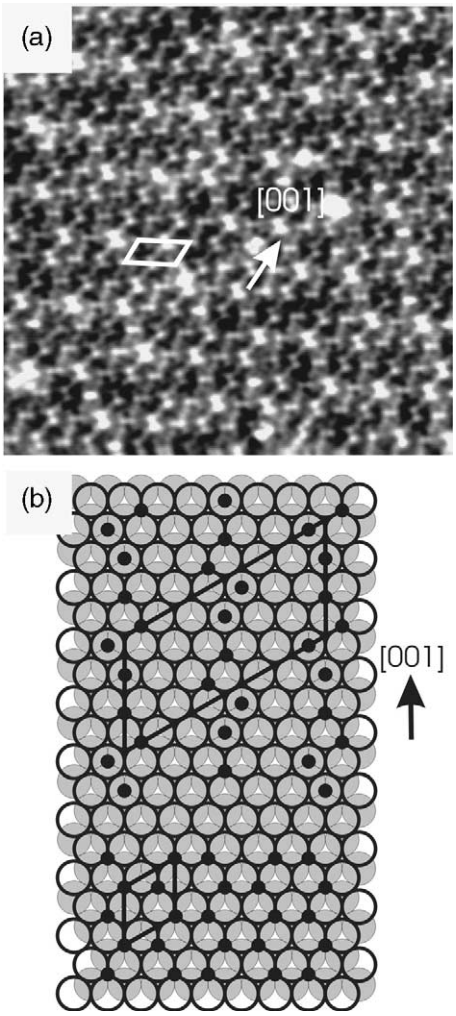

Fig. 3. (a) STM constant current image (20×20 nm^2, $V_s = -1.9$ V, $I_t = -2.54$ nA) depicts Al ions in a zigzag–stripe structural arrangement along the [0 0 1] direction of FeAl(1 1 0). (b) Zigzag–stripe structure is shown on the upper part of the ball model and a pure octahedral structure is included (lower) to compare the unit cells drawn with solid line.

4. Conclusion

The atomic and electronic structure of ultra-thin aluminum oxide films formed on the FeAl(1 1 0) surface has been studied with STM. Upon annealing above 1125 K, the clean surface reconstructs into an incommensurate structure consistent with a $FeAl_2$ stoichiometry confined to the outermost layer. Upon saturating this surface with oxygen, an ordered ultra-thin aluminum oxide film is formed, in direct equivalence with previous studies on low-index surfaces of NiAl. At this coverage, the incommensurate diffraction spots of the clean reconstructed surface have disappeared, implying that the substrate surface does not retain its reconstructed phase. Furthermore, the Al ions imaged by STM were assumed to be nearly in the same plane as the oxygen anions, necessary for electroneutrality, which is in agreement with theoretical calculations performed by Jennison et al. on Al_2O_3(0 0 1)/Al(1 1 1). Confirming the previous calculated electronic structure of Al_2O_3, we asserted that due to limited thickness of the thin oxide film and rearrangement of Al ions, a LDOS of aluminum and oxygen resided in the region of the bulk band gap of the oxide. A combination zigzag and stripe structure of equal octahedrally and tetrahedrally coordinated Al ions was observed.

Acknowledgements

We would like to acknowledge the staff of CAMD for their support in the photoemission studies and G.W. Ownby and J.F. Wendelken of the Solid State Division of ORNL for the support in the crystal preparation and STM studies, respectively. Research at ORNL was sponsored by the Department of Energy managed by UT-Battelle, LLC under contract DE-AC05 00OR22725. The research was also supported by U.S. DOE contract no. DE-FG02-98ER45712.

References

[1] V.E. Henrich, P.A. Cox, The Surface Science of Metal Oxides, Cambridge University Press, Cambridge, 1994.
[2] V.E. Henrich, Rep. Prog. Phys. 48 (1985) 1481.
[3] R. Franchy, Surf. Sci. Rep. 38 (2000) 195.
[4] U. Bardi, A. Atrei, G. Rovida, Surf. Sci. 268 (1998) 87.
[5] S.G. Addepalli, B. Ekstrom, N.P. Magtoto, J.-S. Lin, J.A. Kelber, Surf. Sci. 442 (1999) 385.
[6] R. Franchy, M. Wutting, H. Ibach, Surf. Sci. 189/190 (1987) 438.
[7] R. Franchy, J. Masuch, P. Gassmann, Appl. Surf. Sci. 319 (1994) 95.
[8] R.M. Jaeger, H. Kuhlenbeck, H.-J. Freund, M. Wutting, W. Hoffmann, R. Franchy, H. Ibach, Surf. Sci. 259 (1991) 235.
[9] J. Libuda, F. Winkelmann, M. Bäumer, H.-J. Freund, Th. Bertrams, H. Neddermeyer, K. Müller, Surf. Sci. 318 (1994) 61.
[10] H. Graupner, L. Hammer, K. Heinz, D.M. Zehner, Surf. Sci. 380 (1997) 335.
[11] F. Besenbacher, Rep. Prog. Phys. 59 (1996) 1737.
[12] Landolt-Börnstein, Crystallograhic and Thermodynamic Data of Binary Alloys, New Series, iV/5a, Phase Equilibria, Springer, Berlin, 1991.
[13] W. Köster, T. Gödecke, Z. Metallkd. 71 (1980) 765.
[14] H. Graupner, L. Hammer, K. Müller, D.M. Zehner, Surf. Sci. 322 (1995) 103.
[15] L. Hammer, H. Graupner, V. Blum, K. Heinz, G.W. Ownby, D.M. Zehner, Surf. Sci. 412 (1998) 69.
[16] A.P. Baddorf, S.S. Chandavakar, Phys. B. Cond. Mat. 221 (1996) 141.
[17] D.R. Lide, Handbook of Chemistry and Physics, CRC Press, Boca Raton, 1994.
[18] K.H. Hansen, T. Worren, E. Lægsgaard, F. Besenbacher, I. Stensgaard, Surf. Sci. 475 (2001) 96.
[19] Th. Bertrams, A. Brodde, H. Neddermeyer, J. Vac. Sci. Technol. B 12 (1994) 2122.
[20] C.L. Pang, H. Raza, S.A. Haycock, G. Thorton, Phys. Rev. B 65 (2002) 201401.
[21] D.R. Jennison, C. Verdozzi, P.A. Schultz, M.P. Sears, Phys. Rev. B 59 (1999) 15605.
[22] R. Dupree, M.H. Levis, M.E. Smith, Philos. Mag. A 53 (1986) L17.
[23] V. Jayaram, C.G. Levi, Acta Metall. 37 (1989) 569.
[24] B. Ealet, M.H. Elyakhloufi, E. Gillet, M. Ricci, Thin Solid Films 250 (1994) 92.
[25] D.R. Jennison, A. Bogicevic, Surf. Sci. 464 (2000) 108.